

Electro-osmotic flow in two-dimensional charged micro- and nanochannels

By S. BHATTACHARYYA¹, Z. ZHENG² AND A. T. CONLISK^{3†}

¹Department of Mathematics, Indian Institute of Technology, Kharagpur, India

²Biomedical Engineering Center, The Ohio State University, Columbus, OH 43210, USA

³Department of Mechanical Engineering, The Ohio State University, Columbus, OH 43202, USA

(Received 18 August 2004 and in revised form 23 March 2005)

In this work the electro-osmotic flow in a rectangular channel such that the channel height is comparable to its width is examined. Almost all previous work on the electro-osmotic flow in a channel has been for the case where the channel width is much greater than the channel height and the flow is essentially one-dimensional and depends only on channel height. We consider a mixture of water or another neutral solvent and a salt compound such as sodium chloride for which the ionic species are entirely dissociated. Results are produced for the case where the channel height is much greater than the electric double layer (EDL) (microchannel) and for the case where the channel height is of the order of the width of the EDL (nanochannel). Both symmetric and asymmetric velocity, potential and mole fraction distributions are considered, unlike previous work on this problem. In the symmetric case where all quantities are symmetric about the centreline, the velocity field and the potential are identical as in the parallel-plate one-dimensional case. In the asymmetric case corresponding to different wall potentials, the velocity and potential can be vastly different and reversed flow can occur. The results indicate that the Debye layer thickness is not a good measure of the actual width of the electric double layer. The binary results are shown to compare well with experiment and asymptotic solutions are also obtained for the case of a three-component mixture which may be applied to biomolecular transport.

1. Introduction

In this paper, we consider the electro-osmotic flow problem in a rectangular channel whose width and height are comparable. We consider an aqueous solution and a salt compound such as sodium chloride. For strong electrolytes, the salt component will be entirely dissociated so that nominally, the mixture has three components: undissociated water, and positive and negative ions making up the salt component.

Almost all of the previous work on this problem has been for parallel-plate channels where the height of the channel is much smaller than the width. If the channel walls are charged, there is an induced electric potential due to the surplus of counter ions near the wall. In this case there is no bulk motion of the fluid in the channel. If electrodes are placed upstream and downstream in the desired flow direction, bulk motion of the fluid will occur. The electro-osmotic problem for very small channel heights of the order of the electric double layer has been investigated by a number

† Author to whom correspondence should be addressed: conlisk.1@osu.edu

of authors (Verwey & Verbeek 1948; Burgeen & Nakache 1964; Rice & Whitehead 1965; Levine 1975a; Qu & Li 2000). Much of this work requires the Debye–Huckel approximation for small potentials to be valid and all of the aforementioned work requires symmetry about the centreline of the parallel plate channel. In addition, all of the previous work mentioned above requires that the ionic species be pairs of ions of equal and opposite valence. Electro-osmotic flow in nanoscale tubes has also been examined experimentally (Kemery, Steehler & Bohn 1998) and analytically (Levine 1975b).

Conlisk *et al.* (2002) solve the problem for the ionic mole fractions and the velocity and potential for strong electrolyte solutions and consider the case where there is a potential difference in the direction normal to the channel walls corresponding in some cases to oppositely charged walls. They find that under certain conditions reversed flow may occur in the channel which can significantly reduce the flow rate. The validity of the Debye–Huckel approximation is investigated by Conlisk (2005).

Rectangular channels of the type considered here have been investigated by Yang & Li (1997) and Andreev, Dubrovski & Stepanov (1997). In both cases, symmetric pairs of ionic species are considered. Yang & Li (1997) solve the fully nonlinear problem using a Green’s function approach and include a pressure-driven component which interacts with the electro-osmotic component. They also study the electroviscous effect. Andreev *et al.* (1997) invoke the Debye–Huckel approximation valid for small potentials and calculate the solution for the velocity by Fourier series methods. They are primarily concerned with channels on the micron scale and all of these papers are for the case of very thin electric double layers. While different ζ -potentials on different walls are considered, no reversed flow is found to occur. Neither of these papers consider an asymptotic analysis valid for thin double layers, nor the presence of multivalent ions in a mixture of more than two components.

In this paper we examine the behaviour of the flow in a rectangular channel of a mixture consisting of two or three possibly multivalent ionic species plus an aqueous solvent; we consider for example, both a NaCl–H₂O mixture and a mixture of three electrolytes having several different valences, under the action of an electric field in the primary direction of motion. However, the methods described here may be applied to mixtures having an arbitrary number of ionic constituents of arbitrary valence. In particular, we calculate the mole fractions of the ions and the potential and velocity and consider the case of both overlapping and thin double layers. In the latter portion of the paper, we consider the case of a three-component mixture in the asymptotic limit of a thin electric double-layer thickness. We need not assume symmetry about the centreline and so we consider both symmetric and asymmetric boundary conditions on the potential. We consider the case of negatively charged walls, as is common with silica at a neutral pH, and so we expect a surplus of cations near the wall, while in the case of a positively charged wall, we would expect a surplus of anions.

The electro-osmotic flow problem is driven by the presence of the electric double layer (EDL) near the surfaces of the channel. The electric double layer is intrinsic to the system since the walls are charged resulting in a non-zero electric potential and hence an electric field. Bulk fluid motion is then created by the insertion of electrodes upstream and downstream. The Debye-layer thickness is defined by

$$\lambda = \frac{\sqrt{\epsilon_e RT}}{F I^{1/2}}, \quad (1.1)$$

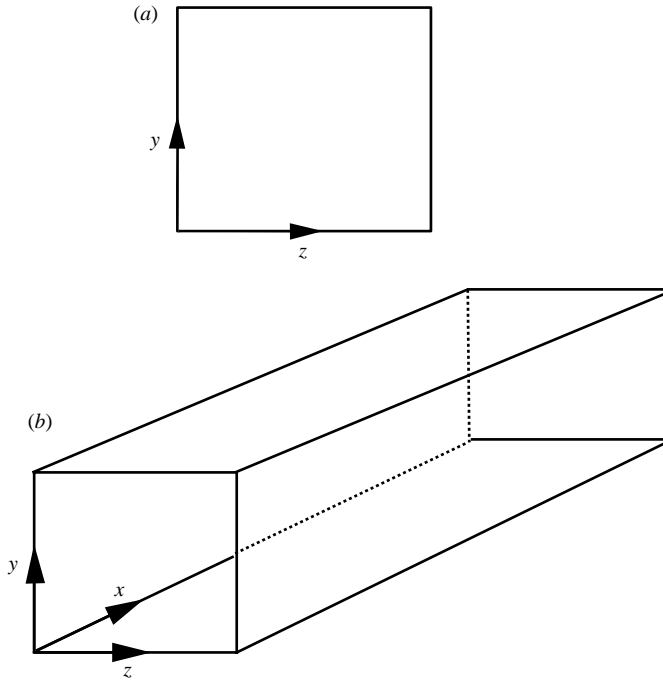


FIGURE 1. Geometry of the channel. u , v and w are the fluid velocities in the x , y and z directions.

where F is Faraday's constant, ϵ_e is the electrical permittivity of the medium, I is the ionic strength, R is the gas constant, z_i is the valence of species i and T is the temperature. If the electric double layer is thin compared with the channel dimensions the problem for the electric potential and the mole fraction of the ions is a singular perturbation problem and the fluid away from the electric double layers is electrically neutral. In this case, the actual thickness of the EDL, defined as the position where the velocity reaches 99% of its value in the core is approximately $\delta_{DL} = d\epsilon$ where $\epsilon = \lambda/h$ and d is a number which depends on the ionic strength at the wall. Here, δ_{DL} is a dimensionless length scaled on the channel height h , similar to the dimensionless boundary-layer thickness in classical fluid mechanics. Typically, for a relatively concentrated mixture, $d \sim 5$ as for the Blasius boundary layer. We also consider the case where $\epsilon \sim 1$ in which case the channel height is of the order of the EDL thickness and the layers on the walls are overlapping. For extremely dilute mixtures, the EDL thickness can be of the order of 100 nm. We assume that the temperature is constant.

The purpose of the present paper is to present the theory of electro-osmotic flow in a two-dimensional channel for the case where the Debye–Hückel approximation is not valid. The geometry is depicted on figure 1. The plan of the paper is as follows. In §2, the governing equations are derived; the flow field, the electric field and the mass transfer problems are fully coupled. In the following section, we solve the equations both for the case of a double layer that is much thinner than the channel height and $\lambda/h = O(1)$, and calculate the volume flow rate through the channel; as noted above, the width of the channel $W \sim h$. We will also investigate the differences between one-dimensional and two-dimensional flow specifically for those cases that are symmetric about the centreline.

2. Governing equations

Let us now consider the mass transport in a liquid mixture of three components, say water and a salt such as sodium chloride flowing in the channel depicted in figure 1. The electric field in general can be composed of two components: an externally imposed electric field, E_0 , and a local electric field present near the solid surfaces of the channel corresponding to the presence of an electric double layer. In dimensional form, the molar flux of species A for a dilute mixture is a vector and given by (Bird, Stewart & Lightfoot 1960)

$$n_A = -cD_{AB}\nabla X_A + u_A z_A F X_A \mathbf{E}^* + c X_A \mathbf{u}^* . \tag{2.1}$$

Here, D_{AB} is the diffusion coefficient, c is the total concentration, X_A is the mole fraction of species A , which can be either the anion or the cation, u_A is the mobility, z_A is the valence, \mathbf{E}^* is the total electric field and \mathbf{u}^* is the mass average velocity of the fluid. The mobility u_A is defined by the Nernst–Planck equation as $u_A = D_{AB}/RT$. In the present paper, we assume that the electrolyte concentration is small enough that the only interactions are between the electrolyte and solvent, so that we write $D_{AB} = D_A$.

The coordinates (x, y, z) are non-dimensional; for example, $x = x^*/L$ and the scaling lengths in the three directions are (L, h, W) . Also (u, v, w) are the dimensionless velocities in each of the coordinate directions (x, y, z) ; for example $u = u^*/U_0$ where u^* is dimensional. Here, $\epsilon_1 = h/L$ and $\epsilon_2 = h/W$. We assume $h, W \ll L$ so that ϵ_1 is small; here z_A is the valence of species A . $Re = U_0 h/\nu$ is the Reynolds number and $Sc = \nu/D_{AB}$ is the Schmidt number, where ν is the kinematic viscosity and $U_0 = \epsilon_e E_0 \phi_0/\mu$ is the velocity scale (Conlisk *et al.* 2002).

We assume that the dimensional potential is of the form

$$\phi^* = -E_0 x^* + \phi_1^*(y^*, z^*),$$

where it can be seen that ϕ_1^* is the perturbation potential from the externally applied field.

Note that

$$E_0 = -\frac{\partial \phi^*}{\partial x^*}.$$

Non-dimensionalizing the equation for the potential as above, dropping the 1 on the perturbation potential and assuming $\phi_{y0} = \phi_{z0} = \phi_0$, $\phi = \phi^*/\phi_0$,

$$\epsilon^2 \left(\frac{\partial^2 \phi}{\partial y^2} + \epsilon_1^2 \frac{\partial^2 \phi}{\partial x^2} + \epsilon_2^2 \frac{\partial^2 \phi}{\partial z^2} \right) = -\beta \sum_{i=1}^N z_i X_i, \tag{2.2}$$

where here ϕ is the dimensionless perturbation potential. Also $\beta = c/I$ where c is the total concentration and I is the ionic strength. Note that (2.2) treats the ionic species as point charges. The channel is assumed long compared to its width and breadth, i.e. ϵ_1 is small and $\epsilon_2 = O(1)$. The largest inertial terms in the mass transfer equations are of the order of $ReSc$ and since the Schmidt number is large in liquids, and of the order of 10^3 , the calculations here will be valid for all Reynolds numbers of $O(10^{-4})$ and smaller. In this case, the governing equations become, to leading order, and for a binary mixture,

$$\frac{\partial v}{\partial y} + A \frac{\partial w}{\partial z} = 0, \tag{2.3}$$

$$\epsilon^2 \left(\frac{\partial^2 u}{\partial y^2} + A^2 \frac{\partial^2 u}{\partial z^2} \right) = \epsilon_1 \epsilon^2 \frac{\partial p}{\partial x} - \beta(z_g g + z_f f), \quad (2.4)$$

$$\epsilon^2 \left(\frac{\partial^2 v}{\partial y^2} + A^2 \frac{\partial^2 v}{\partial z^2} \right) = \epsilon^2 \frac{\partial p}{\partial y} + \Lambda \beta \frac{\partial \phi}{\partial y} (z_g g + z_f f), \quad (2.5)$$

$$\epsilon^2 \left(\frac{\partial^2 w}{\partial y^2} + A^2 \frac{\partial^2 w}{\partial z^2} \right) = \epsilon^2 A \frac{\partial p}{\partial z} + \Lambda \beta \frac{\partial \phi}{\partial z} (z_g g + z_f f), \quad (2.6)$$

$$\epsilon^2 \left(\frac{\partial^2 \phi}{\partial y^2} + A^2 \frac{\partial^2 \phi}{\partial z^2} \right) = -\beta(z_g g + z_f f), \quad (2.7)$$

$$\epsilon^2 \left(\frac{\partial^2 g}{\partial y^2} + A^2 \frac{\partial^2 g}{\partial z^2} \right) = \beta z_g g (z_g g + z_f f) - \epsilon^2 z_g \left(\frac{\partial \phi}{\partial y} \frac{\partial g}{\partial y} + A^2 \frac{\partial \phi}{\partial z} \frac{\partial g}{\partial z} \right), \quad (2.8)$$

$$\epsilon^2 \left(\frac{\partial^2 f}{\partial y^2} + A^2 \frac{\partial^2 f}{\partial z^2} \right) = -\beta z_f f (z_g g + z_f f) - \epsilon^2 z_f \left(\frac{\partial \phi}{\partial y} \frac{\partial f}{\partial y} + A^2 \frac{\partial \phi}{\partial z} \frac{\partial f}{\partial z} \right), \quad (2.9)$$

where we have written the cation mole fraction as g and the anion mole fraction as f and $A = \epsilon_2$ is the aspect ratio of the channel. Also $\Lambda = \phi_0 / E_0 h$. The parameter $\epsilon = \lambda / h$, where λ is the Debye length. In the present investigation, we focus primarily on the flow along the direction of the externally imposed electrical body force, although the possibility of spanwise(w) and vertical(v) velocities is also explored.

To summarize, we have a series of seven equations in seven unknowns to solve for the three-dimensional velocity field, the pressure, the potential and the two mole fractions; the boundary conditions are given by

$$\phi = 0; f = f^0, g = g^0 \text{ at } y = 0, \quad z = 0, \quad (2.10)$$

$$\phi = \phi^1; f = f^1, g = g^1 \text{ at } y = 1, \quad z = 1, \quad (2.11)$$

$$u, v, w = 0 \text{ at } y = 0, z = 0, \quad y = 1, z = 1. \quad (2.12)$$

For this simplified case, the dependent variables are functions of eight separate parameters in addition to the three coordinate directions: ϵ , A , β , Λ , g^0 , g^1 , f^0 and f^1 . Consider the symmetric case here where $g^0 = g^1$ and $f^0 = f^1$. Then there are six independent parameters. We can reduce this number by recognizing that β and ϵ always occur in the ratio ϵ^2 / β . Further, rescaling the mole fractions on the value g^0 , $G = g / g^0$, $F = f / g^0$ then the governing equations are invariant to the rescaling of the mole fractions and the main parameter is now $\delta^2 = \epsilon^2 / \beta g^0$; the other parameters are channel aspect ratio A and $\gamma = f^0 / g^0$. The boundary conditions now become

$$\phi = 0; F = \gamma; G = 1 \text{ at } y = 0, \quad z = 0, \quad (2.13)$$

$$\phi = \phi^1; F = \gamma; G = 1 \text{ at } y = 1, \quad z = 1, \quad (2.14)$$

and we have cut the number of parameters in half. In the asymmetric case where the electric potentials at $y=0$ and $y=1$ are not the same, there are three more parameters corresponding to two sets of the ratio of wall mole fractions at $y=1$ to g^0 and the value of the potential at $y=1$.

Note that δ is a function of both geometry and concentration. This is an important observation since it allows comparison of small channels at larger concentrations with larger channels at smaller concentrations. For example, a value of $\delta = 0.075$

corresponds both to a cation concentration of 0.15 mM with $\lambda = 34$ nm and a channel dimension of 470 nm and to a cation concentration of 0.15 M and a channel dimension of 15 nm with $\lambda = 1$ nm. Thus because physical limitations prevent the measurement of velocity and concentration profiles under approximately $h = 200$ nm (Sadr *et al.* 2004), modelling can be used to relate flows in nanoscale conduits to those in microscale conduits where these profiles can be measured.

For computational purposes we must derive an equation for the pressure. As in classical computational fluid dynamics, we differentiate the momentum equations and after some algebra, we obtain a Poisson equation for the pressure in the form,

$$\delta^2 \left(\frac{\partial^2 P}{\partial y^2} + \frac{\partial^2 P}{\partial z^2} \right) = \Lambda \left(\frac{\partial^2 g}{\partial y^2} + A^2 \frac{\partial^2 g}{\partial z^2} + \frac{\partial^2 f}{\partial y^2} + A^2 \frac{\partial^2 f}{\partial z^2} \right). \quad (2.15)$$

We now consider the case where $\delta \sim \epsilon \ll 1$ before considering full numerical solutions.

3. Asymptotic solution for binary electrolytes of arbitrary valence

In the case where $\delta \ll 1$, we can obtain analytical solutions for the flow within the EDL. This situation is a classical singular perturbation problem. Consider the case of two species of arbitrary valence, with say $X_1 = g$, $X_2 = f$. It is easier to start in the region near the walls. For example, near $y = 0$ we set $Y = y/\delta$. Then using the governing equations for the mole fractions, we find that for g ,

$$\frac{\partial}{\partial Y} \left(\frac{\partial g}{\partial Y} + z_g g \frac{\partial \phi}{\partial Y} \right) = 0. \quad (3.1)$$

This is simply the one-dimensional Boltzmann equation which has the well-known solution

$$g = g^0 \exp(-z_g \phi), \quad (3.2)$$

where we have assumed that $\phi^0 = 0$. The solution for f follows immediately,

$$f = f^0 \exp(-z_f \phi). \quad (3.3)$$

To obtain the matching conditions, we find that the outer solution for the electrolyte of positive valence, g_o , must be

$$g_o = \lim_{Y \rightarrow \infty} g = g^0 \exp(-z_g \phi_o), \quad (3.4)$$

where the subscript 'o' denotes 'outer'. Similarly,

$$f_o = \lim_{Y \rightarrow \infty} f = f^0 \exp(-z_f \phi_o). \quad (3.5)$$

In the core region, it is obvious that for $\epsilon \ll 1$,

$$f_o = -\frac{z_g}{z_f} g_o. \quad (3.6)$$

Thus we have from the limit of the inner solution,

$$z_g g^0 \exp(-z_g \phi_o) = z_f f^0 \exp(-z_f \phi_o), \quad (3.7)$$

and solving for the outer solution ϕ_o we find that

$$u_o = \phi_o = \frac{1}{z_g - z_f} \ln \frac{-z_g g^0}{z_f f^0}. \quad (3.8)$$

This is the one-dimensional result for the symmetric case generalized to arbitrary valence (Conlisk *et al.* 2002). The subscript o again denotes the outer solution valid away from the wall. Clearly, $z_g \neq z_f$ in order to avoid a singularity. As in the one-dimensional case (Conlisk *et al.* 2002), the result for the mole fraction is

$$f_o = \sqrt{-\frac{z_g}{z_f} g^0 f^0 \exp(-(z_g + z_f) \phi_o)}. \tag{3.9}$$

Now consider the y -momentum equation. The appropriate balance is obtained by considering the continuity equation where it is apparent that $v \sim \delta$. This means that the left-hand side of (2.5) is $O(\delta)$ and the two terms on the right-hand side balance if

$$p = \delta^{-2} p_1 + \dots$$

and thus

$$\frac{\partial p_1}{\partial Y} + \Lambda \frac{\partial \phi}{\partial Y} (g - f) = 0. \tag{3.10}$$

Equation (2.5) becomes

$$\frac{\partial^2 p_1}{\partial Y^2} = \Lambda \left(\frac{\partial^2 g}{\partial Y^2} + \frac{\partial^2 f}{\partial Y^2} \right) \tag{3.11}$$

and it can be shown using the equations for f, g that (3.11) is the differentiated form of (3.10). Integrating and putting $p_1 = 0$ at the surface, we obtain

$$p_1 = \Lambda (g + f) - \Lambda (g^0 + f^0), \tag{3.12}$$

and so there is a pressure gradient generated within the EDL. The scaled version of (2.6) shows that for uniform wall concentrations, the velocity $w = 0$. Clearly in this situation, $v = 0$ from continuity. Note that in the case where the potential is symmetric about the centreline, the equations for the streamwise velocity, u and the potential ϕ are the same and solutions in the inner region can be calculated numerically (Conlisk *et al.* 2002).

Clearly the solution in the boundary layers near $z = 0, 1$ will yield the same solution as in the one-dimensional case and is formally equivalent to the solution on $y = 0$ for the same boundary conditions for aspect ratio $A = 1$. For $A \neq 1$, the boundary layer variable near the sidewalls is $Z = z/\delta A$ and so the effective boundary-layer thickness is different from that on the top and bottom walls. Note that in the case where the potential is symmetric about the centreline, the equations for the streamwise velocity, u and the potential ϕ are the same and solutions in the inner region can be calculated numerically (Conlisk *et al.* 2002).

In the case where there is a potential difference across the channel, the potential can at most be a linear function of y and thus

$$\phi_o = \left(\frac{1}{z_g - z_f} \ln \frac{-z_g g^1}{z_f f^1} - \frac{1}{z_g - z_f} \ln \frac{-z_g g^0}{z_f f^0} \right) y + \frac{1}{z_g - z_f} \ln \frac{-z_g g^0}{z_f f^0}. \tag{3.13}$$

Similarly, the mole fractions can at most be linear and for f we obtain

$$f_o = \left(-\frac{z_g}{z_f} g^1 f^1 \exp(-(z_g + z_f) \phi_o^1) + \frac{z_g}{z_f} g^0 f^0 \exp(-(z_g + z_f) \phi_o^0) \right) y - \frac{z_g}{z_f} g^0 f^0 \exp(-(z_g + z_f) \phi_o^0), \tag{3.14}$$

and the velocity is given by

$$u_o = \phi_o - \phi^1. \tag{3.15}$$

4. Numerical methods

To consider overlapped double layers and in anticipation of extending the results to arbitrary numbers of components of arbitrary valence we compute solutions numerically. For both the symmetric and the asymmetric cases, we use second-order central differences to approximate the derivatives in the governing equations. This procedure leads to a system of nonlinear algebraic equations and Newton's linearization technique is applied to cope with the nonlinearity. In this technique, we solve for the dependent variables in an iterative manner. The recurrence relation between the k and $(k + 1)$ iteration at each grid point is given by

$$X_{i,j}^{k+1} = X_{i,j}^k + DX_{i,j}^k, \quad (4.1)$$

with $i = 2, \dots, N - 1$ and $j = 2, \dots, M - 1$ and $k > 0$. Here $DX_{i,j}^k$ is the error of approximation at the k th iteration and $X_{i,j}$ represents the dependent variables $u_{i,j}$, $\phi_{i,j}$, $f_{i,j}$ and $g_{i,j}$. The system of tridiagonal algebraic equations is solved using line relaxation with an underrelaxation factor. The iteration procedure is repeated until the following convergence criteria are satisfied

$$\max |X_{i,j}^{k+1} - X_{i,j}^k| < \Delta$$

for $i = 2, 3, \dots, N - 1$; $j = 2, 3, \dots, M - 1$, where $\Delta = 10^{-5}$.

For larger values of channel height, $\Delta = 10^{-5}$ was used. In general, four-digit accuracy was achieved in solutions for 81 and 161 points across the channel in all of the variables for all of the runs made. For $h = 20$ nm and above, four-digit accuracy was achieved for 161 and 321 points across the channel.

In order to obtain the results out to 100 nm numerically, we use the solution for the channel of height $h - \Delta h$ and the initial guess for the channel of height h . In general, for smaller channel heights, Δh could be fairly large, but as h increases it is difficult to converge for the larger values of Δh . Thus to reach 100 nm we used a value $\Delta h = 1$ nm.

5. Numerical results for specified wall concentrations

We have produced results for channel heights up to 100 nm = 0.1 μ m. For channel heights larger than about 20 nm, for about a 0.1 M mixture, the asymptotic analysis discussed previously can be used. For small potentials less than about 26 mV we would expect that the Debye–Huckel approximation holds, for which the Poisson–Boltzmann distribution is linearized leading to analytical solutions for the velocity and potential (Andreev *et al.* 1997; Yang & Li 1997). Here, we present results for relatively large differences in mole fraction. In figure 2 are results for the velocity and potential and mole fractions for channel height 5 nm. The concentrations shown here correspond to 0.154 M of the cation and 0.0141 M for the anion. We use the notation (g, f) for the rescaled mole fractions depicted on the figures.

It should be pointed out that this case is near the limit where the finite size of the ions would be expected to become important. The diameter of a water molecule and common univalent ions is about three angstroms; thus the 'liquid' Knudsen number defined as the ratio of a molecular diameter to the channel height is about 0.06. It would be beneficial to compare these continuum results which treat the ions as point charges with molecular dynamics (MD) simulations and this has already been done in one dimension (Zhu *et al.* 2005) where it is shown that wall exclusion effects become important at about $h = 6$ nm or about twenty molecular diameters. However, in the

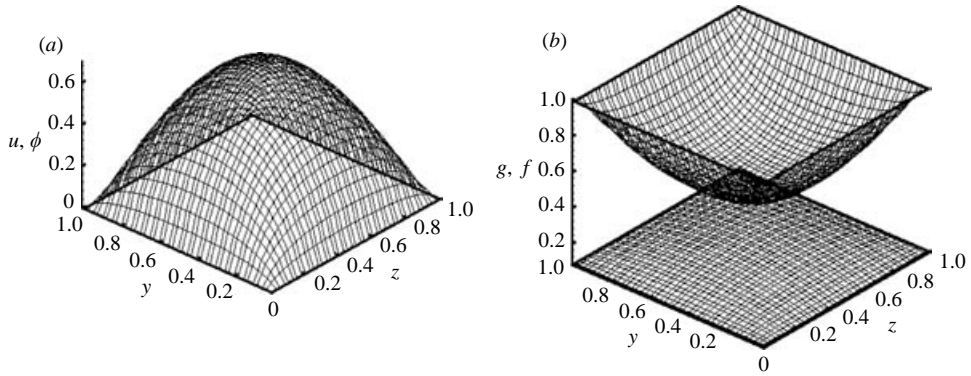


FIGURE 2. The dimensionless velocity and potential along with the mole fraction for $h = 5$ nm; here $\delta = 0.23$, $A = 1$. Here the electric field corresponds to 6 V over a channel of length $L = 3.5 \mu\text{m}$. The mole fractions are scaled on g^0 . (a) Potential and velocity. (b) Rescaled mole fractions for $f^0 = f^1 = 0.000252$ and $g^0 = g^1 = 0.00276$.

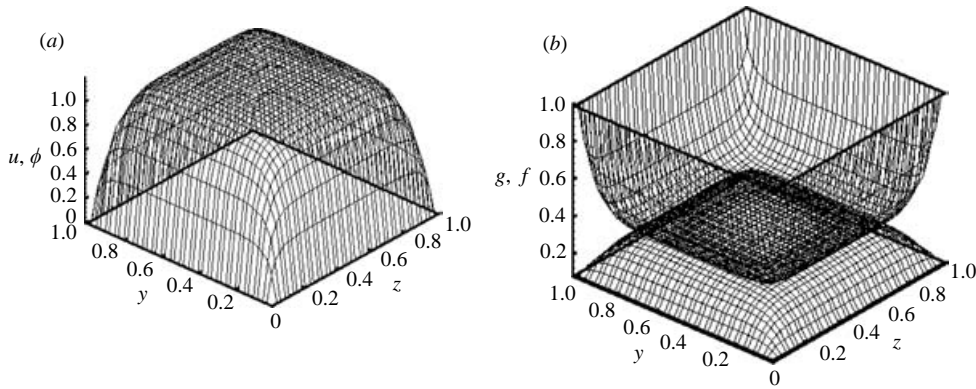


FIGURE 3. Results for the dimensionless velocity and potential along with mole fractions for the case of an NaCl–water mixture. Here the electric field corresponds to 6 V over a channel of length $L = 3.5 \mu\text{m}$; the channel height $h = 25$ nm. The mole fractions are scaled on g^0 . (a) Velocity and potential. (b) Rescaled mole fractions for $f^0 = f^1 = 0.000252$ and $g^0 = g^1 = 0.00276$.

one-dimensional case, the continuum solution is easily adjusted to account for the ion exclusion effects. As in the one-dimensional case (Conlisk *et al.* 2002), the core of the channel is not electrically neutral.

Results for $h = 25$ nm and 50 nm appear in figures 3 and 4. Note that the EDL is extremely thin; by $h = 100$ nm, (figure not shown) the EDL thickness is negligible. The familiar top-hat velocity profile appears as in the one-dimensional result and for these cases where all of the EDLs are thin, the one-dimensional and two-dimensional results for the velocity are equivalent. The value of the potential and velocity in the core is about 1.189 for $h = 50$ nm which is very close to the asymptotic value of $\phi_o = \ln(g^0/f^0)/2 = 1.195$ for monovalent species. The boundary-layer thickness can be defined, as in the classical high-Reynolds-number flow, as the position where the velocity or potential reaches 99 % of its bulk value. The boundary-layer thickness will depend on the molarity and for $h = 25$ nm for the molarities chosen, the boundary-layer thickness is $\delta_{25} = 5.8\epsilon$ and for $h = 50$ nm, $\delta_{50} = 5.7\epsilon$.

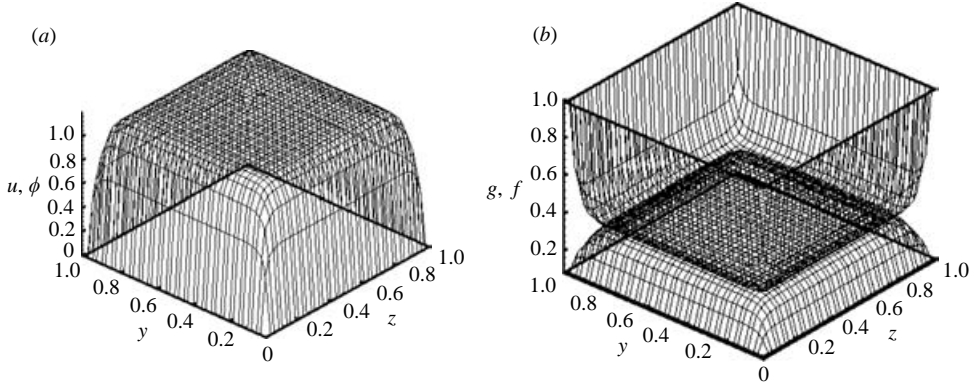
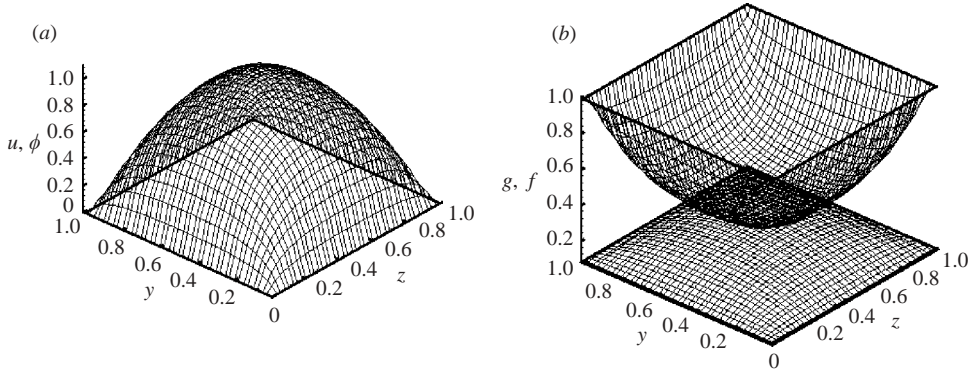
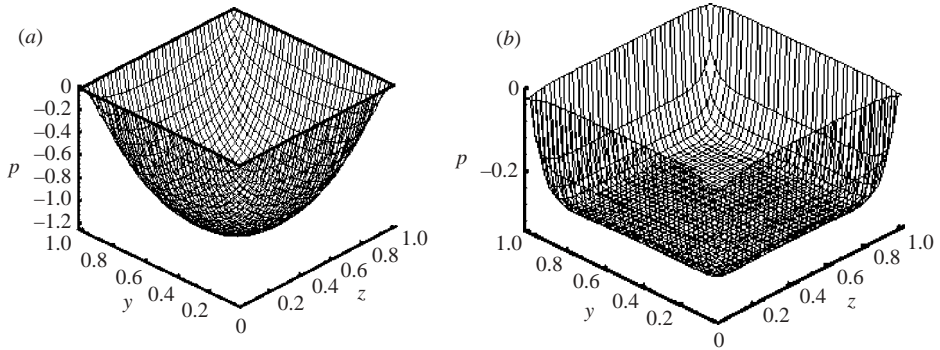
FIGURE 4. As for figure 3, but for $h = 50$ nm.

FIGURE 5. As for figure 3, but for a more dilute mixture of NaCl–water.

FIGURE 6. Pressure distribution for the parameters of figure 2 and 3. (a) $h = 5$ nm; (b) $h = 25$ nm.

In figure 5, results are given for ionic strength 10 times less than in the previous figures for $h = 25$ nm. Here, $\delta = \lambda/h = 0.14$. The results look like a channel much larger at a smaller ionic strength and the EDLs are overlapping for this molarity. A δ value of 0.14 is equivalent to a $1\ \mu\text{m}$ channel at $10\ \mu\text{M}$ concentration.

The pressures for $h = 5$ and 25 nm are shown in figure 6. Here, the pressure is put equal to zero on the boundary and note that the pressure drops in the core and is symmetric about both axes. Here, we note also that the pressure gradients in both

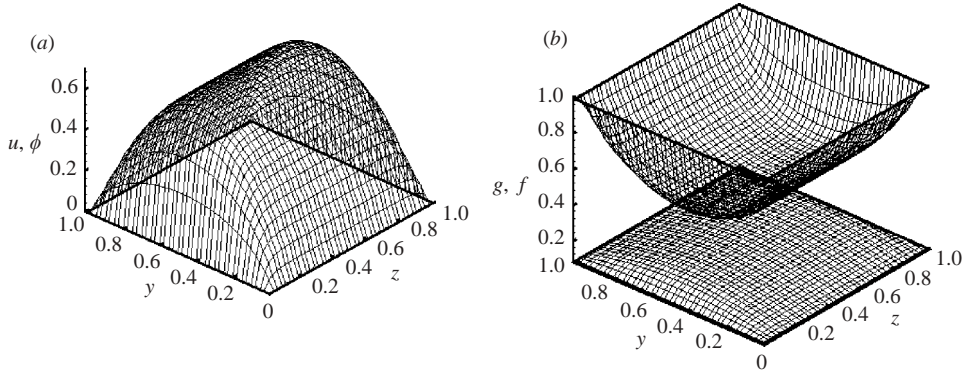


FIGURE 7. Results for the dimensionless velocity and potential along with mole fractions for channel width $W = 20$ nm, $h = 4$ nm so that the aspect ratio $A = 0.2$. Here, $\delta \sim \epsilon = 0.2$. The electric field corresponds to 6 V over a channel of length $L = 3.5$ μm . (a) Velocity and potential. (b) Mole fractions $f^0 = f^1 = 0.000252$ and $g^0 = g^1 = 0.00276$.

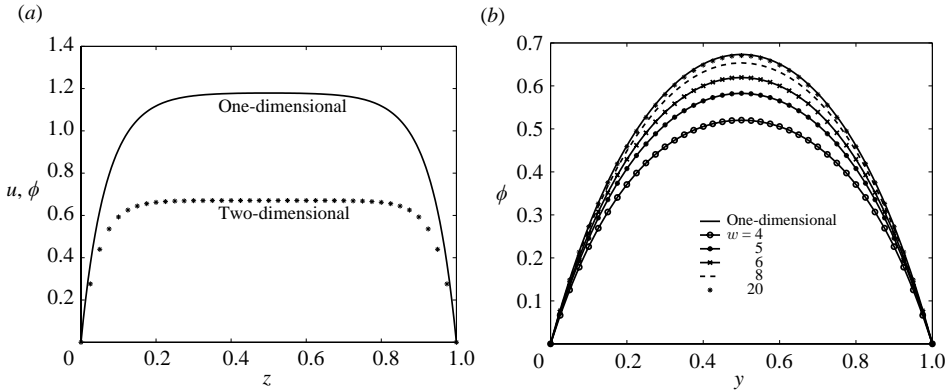


FIGURE 8. (a) Results for the dimensionless velocity and potential for channel width $W = 20$ nm, $h = 4$ nm plotted as a function of spanwise position and compared with the one-dimensional value. The electric field corresponds to 6 V over a channel of length $L = 3.5$ μm . Mole fractions $f^0 = f^1 = 0.000252$ and $g^0 = g^1 = 0.00276$. (b) Plot of the velocity and potential as a function of y for several channel widths.

directions exist because of the presence of the electric double layers on the sidewall and the gradients exist despite the fact that the flow is one-dimensional.

The mole fractions, potential and velocity, are depicted on figure 7 for unequal height and width. Note that the electric double layers are thin near the walls $z = 0, 1$, but overlapping on $y = 0, 1$. This means that one-dimensional models will not be accurate in describing the spanwise behaviour of the potential and velocities and mole fractions. This is shown on figure 8(a). Here, we see that the two-dimensional results are roughly half of the amplitude of the one-dimensional results. Figure 8(b) shows results for the velocity and potential for varying channel width plotted against channel height coordinate y . Note that the one-dimensional result is recovered at a width of about 20 nm. However, the spanwise variation does not match the one-dimensional result even for $W = 20$ nm as shown on figure 8(a).

Asymmetric results are presented on figure 9. The boundary conditions are chosen to correspond to equal electrochemical potential at the walls since there can be no

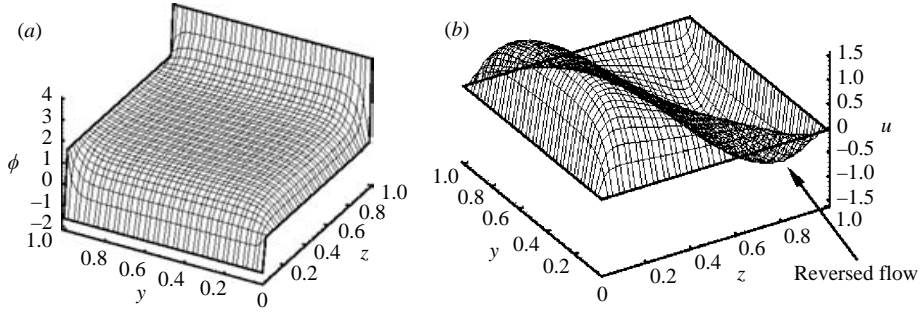


FIGURE 9. Results for (a) the dimensionless potential and (b) velocity along with mole fractions for an asymmetric case. Here the electric field corresponds to 6 V over a channel of length $L = 3.5 \mu\text{m}$; the channel height $h = 20 \text{ nm}$ and aspect ratio $A = 1$. Wall molarity of cation species: $g = 0.154 \text{ M}$ at $y = 0$, $g = 0.033 \text{ M}$ at $y = 1$, $g = 0.724 \text{ M}$, at $z = 0$ and $g = 0.003 \text{ M}$ at $z = 1$; in the same order $f = 0.014 \text{ M}$, 0.066 M , 0.003 M , 0.075 M . The potential at the walls, also in the same order, $\phi = 0, 0.04 \text{ V}, -0.04 \text{ V}, 0.100 \text{ V}$ and the value of $\epsilon = 0.04$.

net flow through the walls. Note the appearance of reversed flow in figure 9 which significantly reduces the flow rate. Thus, adjusting the wall potential can have a significant effect on the transport of species through the channel.

6. Reservoir-channel systems

6.1. Equilibrium considerations

Nanochannel systems are usually connected to upstream and downstream reservoirs in which the electrodes are placed. In experiments, the molarities in the reservoirs are known and the mixture is electrically neutral there; a sketch of a typical device is shown in figure 10. We calculate the wall mole fractions using the requirement that the electrochemical potential in the reservoirs far upstream be the same as the average value at any channel cross-section (Zheng *et al.* 2003). This requirement leads to the Nernst equation (Hunter 1981) which is given by

$$\Delta\Psi = \frac{RT}{z_i F} \ln \frac{c_{iR}}{\bar{c}_{iC}} \quad (i = 1, \dots, N), \quad (6.1)$$

where c_{iR} and \bar{c}_{iC} are the average values of the concentration of species i in the reservoir and the fully developed region within the channel, respectively.

We assume a negatively charged wall, as is customary for a silicon channel in which the negative charge is due to deprotonated silanol groups. Then electroneutrality in the channel requires

$$z_f c_f + \sum_i z_i \bar{c}_{iC} = 0, \quad (6.2)$$

where z_f and c_f are the valence and the concentration of the fixed charges on the wall. Electroneutrality in the reservoir requires

$$\sum_i z_i c_{iR} = 0, \quad (6.3)$$

where usually in experiments, c_{iR} is known for each species. Equations (6.1) and (6.2) are $N + 1$ equations in $N + 1$ unknowns for the average molar concentrations in the channel and the Nernst potential $\Delta\Psi$.

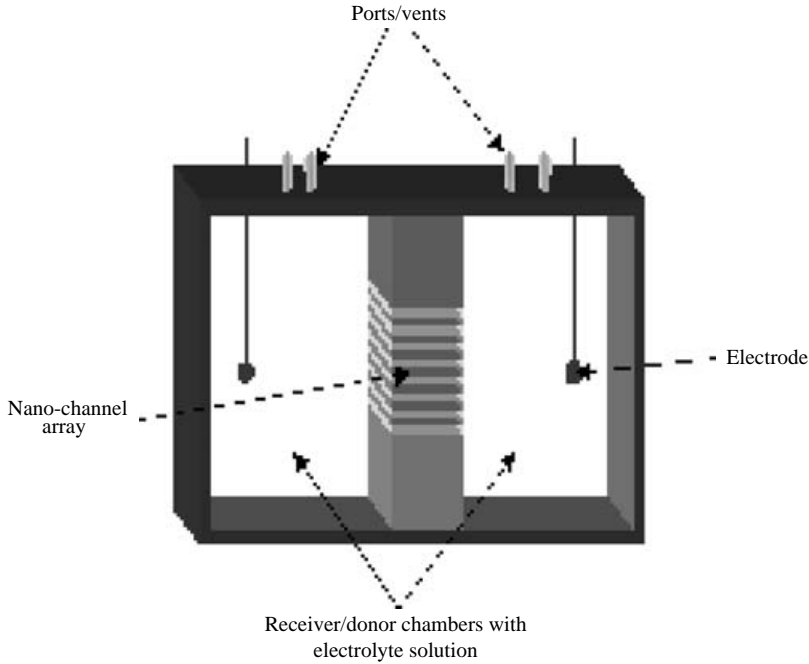


FIGURE 10. Nanopump system (iMEDD, Columbus, Ohio) showing upstream and downstream reservoirs. The molarity (i.e. ionic strength is assumed known in the reservoir).

If the volume of the reservoir is much larger than the volume of the channels, as is the case in practice, then the concentration in the reservoir will be fixed at the value of the concentration prior to the initiation of flow into the reservoir. To obtain each of the average concentrations in the channel, we equate the Nernst potential for each of the species which leads to

$$\bar{c}_{iC} = \left(\frac{\bar{c}_{1C}}{c_{1R}} \right)^{z_i/z_1} c_{iR}. \tag{6.4}$$

where species 1 is, say, the most populous ionic species. Substituting into (6.2) we have

$$z_f c_f + z_1 \bar{c}_{1C} + \sum_{i=2}^N \frac{z_i c_{iR}}{(c_{1R})^{z_i/z_1}} (\bar{c}_{1C})^{z_i/z_1} = 0, \tag{6.5}$$

This is a single equation for the average concentration of species 1 in the channel \bar{c}_{1C} , assuming the surface charge density is known.

To be dimensionally consistent in (6.5), the surface charge density should be converted to $\text{mol}\cdot\text{l}^{-1}$ (M). To do this we assume that the charges are uniformly distributed and the result is

$$c_f = \frac{A\sigma}{1000V_0F}, \tag{6.6}$$

where A is the surface area and V_0 is the volume. The factor 1000 converts m^3 to litre.

The average concentration in the channel is defined in dimensional form as

$$\bar{c}_i = \frac{1}{h} \int_0^h c_i dy^*, \quad (6.7)$$

and in non-dimensional form, dividing by the total concentration of the mixture, we have

$$\bar{X}_i = \int_0^1 X_i dy \quad (6.8)$$

where X_i is the mole fraction and for example, $\bar{X}_i = \bar{g}$ for the cation and $\bar{X}_i = \bar{f}$ for the anion in a binary electrolyte mixture. Since the governing equations are nonlinear and iteration is required anyway, we iterate on the wall mole fractions as well. The procedure is the following. At the first iteration, the wall mole fraction is assumed to be the average mole fraction as calculated above. After convergence of the governing equations, the average mole fraction is calculated from (6.8). Clearly, the only way that these two quantities can be equal is if the mole fractions across the channel are constant. This is not the case and so the equations are solved again with the new wall mole fraction defined by the equation, for example for the cation g^0

$$g_{m+1}^0 = g_m^0 \frac{\bar{g}}{g_m},$$

where m denotes the iteration number and \bar{g} is the average value of the mole fraction obtained by the procedure described above and is fixed. The form of this equation is motivated by the fact that a higher value of the average mole fraction will lead to a higher wall mole fraction. The iteration procedure continues until successive iterates of the wall mole fraction differ by less than 10^{-4} .

As mentioned above, the surface charge density is assumed. To check the calculations are consistent with the assumed surface charge density, we recalculate the surface charge density from the formula

$$\sigma = -\frac{\epsilon_e RT}{\epsilon h F} \int_0^1 (g - f) dy. \quad (6.9)$$

If the recalculated charge density is equal to the assumed charge density, the solution is found. If not, the surface charge density is changed and the program is run again. It turns out that there is a unique solution where the assumed surface charge density matches the post-convergence calculated value.

The procedure for calculating the wall mole fractions simplifies in the asymptotic case. For the case of a binary electrolyte, the three unknowns corresponding to the Nernst potential and the two wall mole fractions may be obtained by using the outer solutions of the corresponding quantities; this avoids having to integrate the mole fraction across the channel numerically. In this way, we solve

$$\Delta\psi = \frac{1}{z_f} \ln f^R - \ln f_o, \quad (6.10)$$

$$\Delta\psi = \frac{1}{z_g} \ln g^R - \ln g_o, \quad (6.11)$$

and the electroneutrality condition. It is clear that this procedure may be extended to an arbitrary number of electrolytes of arbitrary valence.

mm	μ_e	μ_m	ζ_e	ζ_m	$\epsilon = \delta$	B ₄ O ₇ (wall)	Na(wall)	σ (C m ⁻²)
0.02	5.51×10^{-4}	6.10×10^{-4}	-0.173	-0.197	2.17×10^{-4}	$< 10^{-6}$	0.028	-0.007
0.2	4.60×10^{-4}	5.30×10^{-4}	-0.138	-0.170	9.85×10^{-5}	$< 10^{-6}$	0.133	-0.0154
2	3.52×10^{-4}	3.43×10^{-4}	-0.098	-0.111	9.60×10^{-5}	2.80×10^{-5}	0.141	-0.0154
20	1.71×10^{-4}	1.74×10^{-4}	-0.054	-0.056	8.59×10^{-5}	0.0023	0.1734	-0.0154

TABLE 1. Mobility and ζ -potential for the ORNL data for the 10.4 $\mu\text{m} \times 26 \mu\text{m}$ channel. Note that in this regime $\delta = \epsilon \ll 1$ so that the asymptotic theory applies. The mobilities are in $\text{cm}^2 \text{V}^{-1} \text{s}^{-1}$ and the ζ -potential is in V.

6.2. Asymptotic results for calculated wall concentrations for binary electrolytes

We present numerical results for the inner region near the wall, using the outer solution values as boundary conditions. The wall mole fractions are calculated based on the procedure just described for a given ionic strength in the upstream reservoir.

Consider first the case of a binary electrolyte system. Figure 11 shows velocity, potential, mole fractions and shear stress for three different square channels plotted against the outer variable. The height of the three channels are 25, 50 and 100 nm. As the channel height increases, note that the EDL becomes thinner, and the familiar top-hat profile, characteristic of electro-osmotic flow in micro-channels, appears.

7. Comparison with experimental data

We have compared the model to two sets of experimental data and the comparisons are very good (Zheng *et al.* 2003). We have also compared the model described here with Sadr *et al.* (2004). Here, we compare the results for the calculated wall mole fraction with the experimental data provided to us by J. M. Ramsey (Oak Ridge National Laboratory, personal communication, 2002) for a rectangular channel. The mixture is a sodium tetraborate–methanol solution with a viscosity of 0.00168 Pa s and a dielectric constant of 59.24, as supplied by Ramsey’s group. The mixture is a 1:1 electrolyte and the molarity in the upstream reservoir ranges from 0.02 mM to 150 mM; the channel is 10.4 $\mu\text{m} \times 26 \mu\text{m}$ as in the Georgia Tech case. The electric double layer is very thin so that asymptotic analysis for calculated wall concentrations is sufficient for the comparison. The experimental data correspond to the average velocity divided by the electric field and this is called the electro-osmotic mobility

$$\mu_{eo} = \frac{\frac{1}{2}U_0 \ln(g^0/f^0)}{E_0},$$

which is the result for the outer velocity given by (3.8). Note that the mobility is independent of the electric field since U_0 is linearly dependent on the electric field. The present model for the case of a thin electric double layer can predict the wall ζ -potential, which is measured by the Ramsey group.

The results are depicted on table 1 for four concentrations in the upstream reservoirs. Note that the wall concentration of the sodium is much greater than that in the reservoir for the more concentrated cases. In the present case, since the EDLs are thin, we can define the ζ -potential as the negative of the value of ϕ in the core. On a dimensionless basis since ϕ denotes the perturbation from the wall potential ($\phi = 0$ at the walls), we have

$$\psi = \zeta + \phi. \quad (7.1)$$

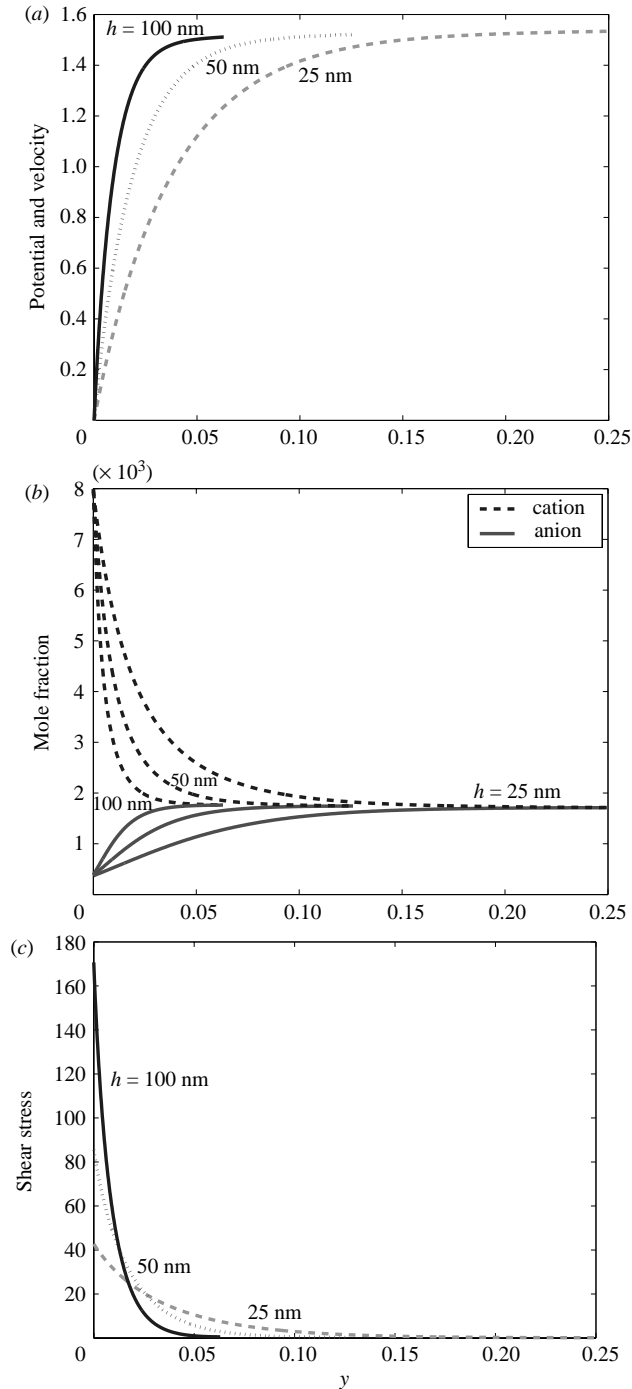


FIGURE 11. Asymptotic results for the dimensionless velocity and potential along with mole fractions (unscaled) and shear stress plotted in the outer variable for the case of an 0.1 M 1:1 electrolyte–water solution in the reservoir. Here the electric field corresponds to 0.05 V over a channel of length $L = 3.5 \mu\text{m}$; the channel height $h = 25, 50, 100$ nm and the reservoir concentration is 2 mM. (a) Velocity and potential. The solid line is the result given by (3.8). (b) Mole fractions. (c) Shear stress.

Defining $\psi = 0$ in the core, results in

$$\zeta^* = -\phi = -\frac{1}{2} \ln \frac{g^0}{f^0}. \tag{7.2}$$

In dimensional form, which is the value that appears in table 1, we have

$$\zeta = -\phi^* = -\frac{1}{2} \frac{RT}{F} \ln \frac{g^0}{f^0}. \tag{7.3}$$

The values compare well with the experimental data for both mobility and ζ -potential.

8. Asymptotic solution for ternary electrolytes

Consider now the case of a three-electrolyte system. Denote the species by (g, f, r) . Then the inner solution is the Poisson–Boltzmann expression as above,

$$X_i = X_i^0 \exp(-z_i \phi), \tag{8.1}$$

where X_i is any one of (g, f, r) . By the same process as for the $N = 2$ case, the outer solutions can be obtained and the results for the symmetric case are

$$g_o = \sqrt{\frac{-z_f g^0 f^0 \exp(-(z_g + z_f)\phi_o)}{z_g + z_r (r^0/g^0) \exp((z_g - z_r)\phi_o)}}, \tag{8.2}$$

$$f_o = \sqrt{\frac{-z_g g^0 f^0 \exp(-(z_g + z_f)\phi_o)}{z_f + z_r (r^0/g^0) \exp((z_f - z_r)\phi_o)}}, \tag{8.3}$$

$$r_o = -\frac{z_f f + z_g g}{z_r}. \tag{8.4}$$

The outer solution for ϕ is given by the solution of the equation

$$\exp((z_g - z_f)\phi_o) = -\frac{z_g g^0}{z_f f^0} - \frac{z_r r^0}{z_f f^0} + \exp((z_g - z_r)\phi_o) \tag{8.5}$$

and $u_o = \phi_o$ in the symmetric case.

We can determine the potential and hence velocity analytically for special cases. If $z_r = z_g$, then

$$\phi_o = \frac{1}{z_g - z_f} \ln \left(\frac{-z_g g^0}{z_f f^0} + \frac{-z_r r^0}{z_f f^0} \right). \tag{8.6}$$

If $z_r = 2, z_g = 1, z_f = -1$, then

$$x^3 - \frac{g^0}{f^0} x - 2 \frac{r^0}{f^0} = 0, \tag{8.7}$$

where $x = \exp(\phi_o)$. These valences are appropriate for a sodium chloride–calcium mixture.

If $z_r = z_g$, we have

$$\phi_o = \frac{1}{z_g - z_f} \ln \left(\frac{z_g (g^0 + r^0)}{-z_f f^0} \right), \tag{8.8}$$

For $z_r = z_f$ or $z_f = z_g$, equation (8.5) can be solved similarly. Next if $z_g + z_f = 2z_r$, the outer solution is given by

$$\phi_o = \frac{1}{z_g - z_r} \ln \left(\frac{-z_r r^0 \pm \sqrt{(z_r r^0)^2 - 4z_g z_f g^0 f^0}}{2z_f f^0} \right). \quad (8.9)$$

Similarly, cases such as $z_g + z_r = 2z_f$ or $z_f + z_r = 2z_g$ can also be solved. Finally, if $2z_g + z_r = 3z_f$, we have

$$\phi_o = \frac{1}{z_g - z_f} \ln \left(\frac{t}{6z_r r^0} - \frac{2z_f f^0}{t} \right), \quad (8.10)$$

where $t = ((-108z_g g^0 + 12\sqrt{3} \sqrt{\frac{4(z_f f^0)^3 + 27(z_g g^0)^2 z_r r^0}{z_r r^0}})(z_r r^0)^2)^{1/3}$.

For the asymmetric case, we find

$$g_o = (g_o^1 - g_o^0) y + g_o^0, \quad (8.11)$$

$$f_o = (f_o^1 - f_o^0) y + f_o^0, \quad (8.12)$$

where, for example, f_o^0 is the limit of the outer solution near $y = 1$

$$f_o^0 = \sqrt{\frac{-z_g g^0 f^0 \exp(-(z_g + z_f)\phi_o^0)}{z_f + z_r(r^0/g^0) \exp((z_f - z_r)\phi_o^0)}}. \quad (8.13)$$

The potential is given in the same way as for $N = 2$ by,

$$\phi_o = (\phi_o^1 - \phi_o^0) y + \phi_o^0. \quad (8.14)$$

The presence of a small amount of a divalent cation in a channel having negatively charged walls has a great effect on the flow (Zheng *et al.* 2003). Figure 12 shows the asymptotic solutions for a 1:1:2 electrolyte mixture for surface charge density $\sigma = -0.0154 \text{ C m}^{-2}$ on the channel wall. Note that the core is still electrically neutral and the electric double layer thins considerably, as before. These results are different from the binary case and a bivalent anion will have little or no effect on the flow compared to the binary case (Zheng *et al.* 2003).

9. Summary

We have produced analytical and numerical results for the electro-osmotic flow in a rectangular channel, both in the case of overlapped double layers and in the case of thin double layers. In cross-section, when the EDL is very thin, the results look similar to those for a one-dimensional or slit-pore channel. However, if the EDLs are overlapping in one direction, one-dimensional flow models will not match the two-dimensional results in the dimension normal to the overlapped dimension. The one-dimensional result in the overlapped direction is recovered at about a channel height of 20 nm for the molarities chosen.

The results show that the Debye-layer thickness is not a good measure of the actual width of the electric double layer. This work has shown that for the molarities considered, the actual dimensional width of the EDL is $\delta^* \sim 6\lambda$, similar to the case in high-Reynolds-number flow.

We have also shown how non-zero wall potentials can produce reversed flow. Thus, chemically treating a wall can have significant effects on the character of the

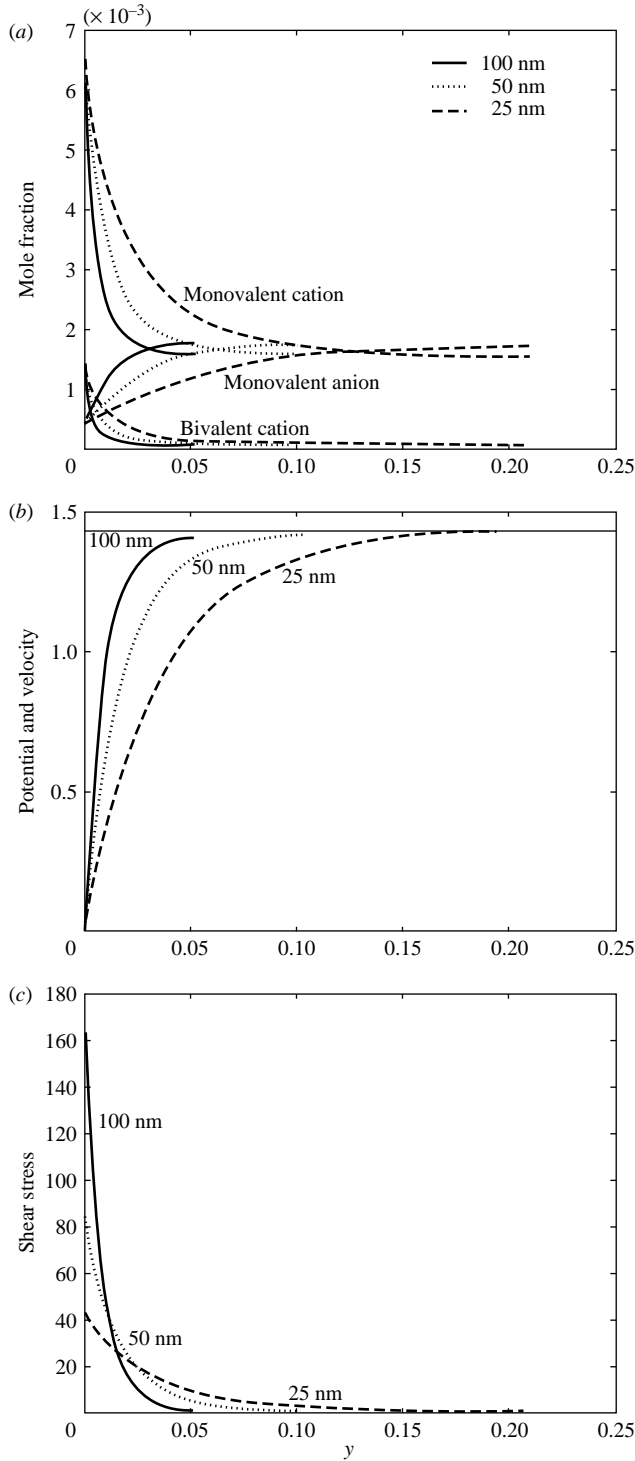


FIGURE 12. Results for a 1:1:2 electrolyte mixture for channel heights $h = 25, 50$ and 100 nm. The width of the channel is $100\ \mu\text{m}$, the surface charge density $\sigma = -0.0154\ \text{C m}^{-2}$, and the concentration of electrolytes in the reservoir is $0.002\ \text{M}$. (a) Mole fractions near the wall. (b) Potential and velocity. (c) Shear stress.

flow. Theoretically, the proper adjustment of wall potential and hence surface charge can result in either mixing or separation and these phenomena are currently being explored.

Analytical solutions for the case of thin double layers characterized by $\delta \sim \epsilon \ll 1$ have been shown to compare well with experimental data for rectangular pores generated by Ramsey (Oak Ridge National Laboratory, personal communication, 2002).

We have produced results for channel heights as small as $h = 5$ nm. This case is near the limit where the finite size of the ions would be expected to become important. The diameter of a water molecule and common univalent ions is about 3 Å; thus the 'liquid' Knudsen number defined as the ratio of a molecular diameter to the channel height is about 0.06. It would be beneficial to compare these continuum results with MD simulations to determine if the two-dimensional case is significantly different from the one-dimensional case where the continuum results can easily be adjusted to match the MD solutions (Zhu *et al.* 2005). It is desirable to have continuum models of nanofluidic devices since nanoscale devices cannot be designed solely by running MD simulations because of the significant computation time required (some weeks).

In addition, many biological problems require the solution for more than two species. This is the case for modelling the transport of a biomolecule in an electrolyte solution. We have presented analytical results for the outer solution for several parameter ranges of the relative valences for the case of three species in the case where $\epsilon \ll 1$. We have also presented numerical results for the inner solution in the case of three species containing a bivalent cation ($z = 2$).

Because of the assumption of fully developed flow, the velocity is one-dimensional and no spanwise motion can occur. Future work will focus on the case where the wall potentials are not uniform, leading to multi-directional flow and the formation of complicated vortical flow patterns.

This work is funded by DARPA under agreement number F30602-00-2-0613. The authors are grateful to the contract monitors Dr Anantha Krishnan (DARPA), Mr Clare Thiem and Mr Duane Gilmour of Air Force Research Lab. (IFTC) for their support. Lei Chen performed the numerical computations for this paper and produced many of the figures. For this work A. T. C. is grateful. The authors are grateful to the referees for their helpful comments.

REFERENCES

- ANDREEV, V. P., DUBROVSKI, S. G. & STEPANOV, Y. V. 1997 *J. Micro. Sep.* **9**, 443–450.
BIRD, R. B., STEWART, W. E. & LIGHTFOOT, E. N. 1960 *Transport Phenomena*. John Wiley.
BURGEEN, D. & NAKACHE, F. R. 1964 Electrokinetic flow in ultrafine capillary slits. *J. Phys. Chem.* **68**, 1084–1091.
CONLISK, A. T. 2005 The Debye–Huckel approximation: its use in describing electroosmotic flow in micro- and nano-channels. *Electrophoresis* **26**, 1896–1912.
CONLISK, A. T., MCFERRAN, JENNIFER, ZHENG, Z. & HANSFORD, D. 2002 Mass transfer and flow in electrically charged micro- and nano-channels. *Analyt. Chem.* **74**, 2139–2150.
HUNTER, R. J. 1981 *Zeta Potential in Colloid Science*. Academic.
KEMERY, P. J., STEEHLER, J. K. & BOHN, P. W. 1998 *Langmuir* **14**, 2884–2889.
LEVINE, S., MARRIOTT, J. R. & ROBINSON, K. 1975a Theory of electrokinetic flow in a narrow parallel-plate channel. *Faraday Trans. II* **71**, 1–11.
LEVINE, S., MARRIOTT, J. R., NEALE, G. & EPSTEIN, N. 1975b Theory of electrokinetic flow in fine cylindrical capillaries at high zeta potentials. *J. Colloid Interface Sci.* **52**, 136–149.

- QU, W. & LI, D. 2000 A model for overlapped EDL fields. *J. Colloid Interface Sci.* **224**, 397–407.
- RICE, C. L. & WHITEHEAD, R. 1965 Electrokinetic flow in a narrow capillary. *J. Phys. Chem.* **69**, 4017–4024.
- SADR, R., YODA, M., ZHENG, Z. & CONLISK, A. T. 2004 An experimental study of electro-osmotic flow in rectangular microchannels. *J. Fluid Mech.* **506**, 357–367.
- VERWEY, E. J. W. & VERBEEK, J. TH. G. 1948 *Theory of Stability of Lyophobic Colloids*. Elsevier.
- YANG, C. & LI, D. 1997 Electrokinetic effects on pressure driven liquid flows in rectangular microchannels. *J. Colloid Interface Sci.* **194**, 95–107.
- ZHENG, Z., HANSFORD, D. J. & CONLISK, A. T. 2003 Effect of multivalent ions on electroosmotic flow in micro and nanochannels. *Electrophoresis* **24**, 3006–3017.
- ZHU, W., SINGER, S. J., ZHENG, Z. & CONLISK, A. T. 2005 Study of electroosmotic flow of a model electrolyte. *Phys. Rev. E* **71**, 041501-1–041501-12.